

Microphthalmia-Associated Transcription Factor (MITF) Regulates Immune Cell Migration into Melanoma

Gabriela Wiedemann, Celina Aithal, Angelina Kraechan, Constanze Heise,
Bruno Cadilha, Jin Zhang, Peter Duewell, Robert Ballotti, Stefan Endres,
Corine Bertolotto, et al.

► **To cite this version:**

Gabriela Wiedemann, Celina Aithal, Angelina Kraechan, Constanze Heise, Bruno Cadilha, et al..
Microphthalmia-Associated Transcription Factor (MITF) Regulates Immune Cell Migration into
Melanoma. *Translational Oncology*, Elsevier, 2019, 12 (2), pp.350-360. 10.1016/j.tranon.2018.10.014 .
inserm-02529778

HAL Id: inserm-02529778

<https://www.hal.inserm.fr/inserm-02529778>

Submitted on 2 Apr 2020

HAL is a multi-disciplinary open access archive for the deposit and dissemination of scientific research documents, whether they are published or not. The documents may come from teaching and research institutions in France or abroad, or from public or private research centers.

L'archive ouverte pluridisciplinaire **HAL**, est destinée au dépôt et à la diffusion de documents scientifiques de niveau recherche, publiés ou non, émanant des établissements d'enseignement et de recherche français ou étrangers, des laboratoires publics ou privés.

Microphthalmia-Associated Transcription Factor (MITF) Regulates Immune Cell Migration into Melanoma



Gabriela M Wiedemann^{*,†,1,2}, Celina Aithal^{*,1,2}, Angelina Kraechan^{*,2}, Constanze Heise^{*,2}, Bruno L Cadilha^{*,2}, Jin Zhang^{*,2}, Peter Duewelle^{*,2}, Robert Ballotti^{†,3}, Stefan Endres^{*,2}, Corine Bertolotto^{†,3} and Sebastian Kobold^{*,2}

^{*}Center of Integrated Protein Science Munich (CIPS-M) and Division of Clinical Pharmacology, Klinikum der Universität München, Lindwurmstrasse 2a, 80337 Munich, Germany; [†]Department of Medicine II, Klinikum rechts der Isar, Technische Universität München, Germany; [‡]INSERM U1065 (Team 1), C3M, Biology and Pathologies of Melanocytes, 151, route Saint Antoine de Ginestière, BP2 3194, 06204 NICE Cedex3

Abstract

Microphthalmia-associated transcription factor (MITF) is a key transcription factor in melanoma development and progression. MITF amplification and downregulation have been observed in a significant proportion of melanoma patients and correlate with clinical outcomes. Here, we have investigated the effect of MITF on melanoma chemokine expression and immune cell attraction. In B16F10 melanoma cells, MITF knockdown reduced expression of CXCL10, with concomitantly decreased attraction of immune cells and accelerated tumor outgrowth. Conversely, overexpression of MITF in YUMM1.1 melanoma cells also led to an increased immune cell attraction *in vitro*. Subcutaneous YUMM1.1 melanomas overexpressing MITF however showed a reduced immune infiltration of lymphocytes and an increased tumor growth. In human melanoma cell lines, silencing of MITF enhanced chemokine production and immune cell attraction, while overexpression of MITF led to lower immune cell attraction. In summary, our results show that MITF regulates chemokine expression in murine and in human melanoma cells, and affects *in vivo* immune cell attraction and tumor growth. These results reveal a functional relationship between MITF and immune cell infiltration, which may be exploited for cancer therapy.

Translational Oncology (2019) 12, 350–360

Introduction

Microphthalmia-associated transcription factor (MITF) is a key transcriptional regulator of the melanocyte cell lineage. It is expressed in 80% of human melanomas and plays an important role in melanoma development and progression [1,2]. MITF is known to regulate a diverse range of transcriptional targets including genes involved in cell cycle arrest, DNA repair, proliferation, survival, and apoptosis as well as cell differentiation [3]. Amplification of MITF is found in 15% to 20% of human metastatic melanomas and has been linked to poor survival [4]. Evidence for the role of changes in MITF levels in melanoma is contradictory. High expression of MITF was found in melanoma relapse after combined BRAF and MEK inhibitor therapy [5]. However, resistance to targeted therapy has also been associated with a decreased expression of MITF [6]. Low levels of MITF are associated with increased invasiveness of melanomas but also with cell senescence, whereas high levels result in differentiation [7–13]. These

findings highlight a central regulatory role of MITF in melanoma cell phenotypic versatility and further underline the importance of understanding its dynamic regulation.

Address all correspondence to: Sebastian Kobold, MD, Division of Clinical Pharmacology, Klinikum der Universität München, Lindwurmstraße 2a, 80337 München.

E-mail: Sebastian.kobold@med.uni-muenchen.de

¹G. M. W. and C. A. contributed equally to this work.

²Member of the German Center of Lung Research.

³Equipe labellisée ARC 2015.

Received 29 October 2018; Accepted 31 October 2018

© 2018 The Authors. Published by Elsevier Inc. on behalf of Neoplasia Press, Inc. This is an open access article under the CC BY-NC-ND license (<http://creativecommons.org/licenses/by-nc-nd/4.0/>).

1936-5233/19

<https://doi.org/10.1016/j.tranon.2018.10.014>

In the past decade, immunotherapy using checkpoint blocking antibodies has changed the treatment of advanced and metastasized melanoma patients [14]. Their effectiveness demonstrates the importance of the immune system in melanoma therapy. However, melanomas in a significant number of patients either do not respond to checkpoint inhibiting antibodies at all or relapse after initial tumor regression. Primary but also secondary treatment failure may result from a lack of effector T cells at the tumor site and is associated with a bad prognosis [15]. Tumors with low immune cell infiltration are frequently referred to as “cold tumors” as opposed to the immune cell-rich “hot tumors” typically responding well to checkpoint blockade. The origins of these different phenotypes are still poorly understood. There is a need for new therapeutic strategies, which convert poorly infiltrated tumors into “hot tumors” [16].

So far, little is known about the effects of MITF on melanoma immune cell infiltration. It has recently been shown that MITF^{low} melanomas display an increased response to exogenous TNF resulting in higher infiltration by CD14⁺ myeloid cells [17]. In addition, in melanoma cells exhibiting a state of senescence due to stable MITF knockdown, an increased expression of the chemokine CCL2 was described favoring proinvasive capacities of melanoma cells in an autocrine manner [12]. These studies suggest that MITF expression levels may affect the melanoma immune landscape. However, no detailed analyses of chemokine expression and immune cell infiltration in melanomas with different MITF expression levels have been performed so far.

In the present work, we investigated the effects of MITF knockdown as well as MITF overexpression in different murine and human melanoma models on chemokine expression and immune cell infiltration, *in vitro* and *in vivo*. We demonstrate that MITF downregulation and MITF upregulation result in changes in the chemokine expression profile on both RNA and protein levels. The differential chemokine expression patterns lead to altered immune cell migration towards tumor cells *in vitro* and correlated with accelerated tumor outgrowth *in vivo* in both conditions. Thus, our data suggest a role for MITF in regulating tumor immune cell infiltration.

Material and Methods

Mice, Cell Lines, and Animal Experiments

C57BL/6 mice were purchased from Janvier (St. Berthevin, France) or Charles River (Wilmington, MA) and were 5 to 12 weeks of age. All animal studies were approved by the local regulatory agency (Regierung von Oberbayern). The human melanoma cell lines WM8 and WM35 and the murine B16F10 melanoma cell line were described previously [18–20]. The murine YUMM1.1 cell line [21] was kindly provided by Dr. Bosenberg (Yale University, USA). Cell lines were cultured in complete DMEM or RPMI medium (PAA Laboratories) and were routinely tested for mycoplasma contamination by MycoAlert Mycoplasma Detection Kit (LONZA). For *in vivo* tumor models, syngeneic tumor cells were injected subcutaneously into the flank of C57BL/6 mice. Mice were sacrificed after 10 to 30 days as indicated. For isolation of tumor-infiltrating lymphocytes, tumors were mechanically disrupted, incubated with 1 mg/ml collagenase and 0.05 mg/ml DNase (both Sigma Aldrich), and passed through a cell strainer. Single-cell suspensions were directly analyzed or layered on a gradient of 44% Percoll (Biochrome, Berlin, Germany) and 67% Percoll prior to centrifugation at 800×g for 30 minutes.

Flow Cytometry

Multicolor flow cytometry was performed using a BD FACS Canto II or BD LSR Fortessa (BD Bioscience, Germany). Flow cytometry antibodies were purchased from Biolegend (San Diego, CA). Anti-human CD8 was purchased from ThermoFisher Scientific (Waltham, MA). The following antibodies were used: anti-human CD3 (OKT3), anti-human CD4 (OKT4), anti-human CD8 (OKT8), anti-human CD19 (HIB19), anti-human CD56 (5.1H11), anti-human CD11c (Bu15), anti-human CD14 (63D3), anti-mouse CD3 (17A2), anti-mouse CD4 (GK1.5), anti-mouse FOXP3 (MF-14), anti-mouse CD8 (52-6.7), anti-mouse B220 (RA3-6B2), anti-mouse NK1.1 (PK136), anti-mouse CD11c (N418), anti-mouse CD11b (M1/70), and Zombie Aqua Fixable Viability Kit.

siRNA Transfection

siRNA against human and murine MITF has been previously published [22,23]. For human siRNA knockdown of MITF, the MITF-specific sequence 5'-CUUGAUGAUCGGAUUCACC-d(TT)-3' and the control sequence 5'-CGU ACG CGG AAU ACU UCG A-3' (LuciferaseGL2) were used. For murine siRNA knockdown, the sequence 5'-GGUGAAUCGGAUCAUAAG-3' (siMITF) and the control sequence 5'-UUCUCCgAACgUgU-CACgUTT-3' (siControl) were used. For transfection, a single pulse of 50 nM siRNA was administered to the cells at 50% to 70% confluency by transfection with 5 µl of Lipofectamine RNAiMAX in opti-MEM medium (both Invitrogen).

Chemokine ELISA

Chemokine protein levels in tumor cell supernatants were determined by R&D DuoSet ELISA for CCL2, CCL5, and CXCL10 (Mouse CCL2/JE/MCP-1, Mouse CCL5/RANTES, Mouse CXCL10/IP-10/CRG-2 DuoSet ELISA, R&D Systems, Minneapolis, MN). Cell free culture supernatants of YUMM1.1 melanoma cells were collected after 48 hours of culture. Culture medium of B16F10 melanoma cells was changed 48 hours after MITF siRNA transfection, and cell free supernatants were collected after another 48 hours of culture and analyzed according to the manufacturer's protocol. Absorbance was measured at 470 nm using the Mithras-Reader (MikroWin program, version 4.41).

Chemokine Protein Arrays

Chemokine protein levels in tumor cell supernatants or tumor lysates were determined by R&D Proteome Profiler Human/Mouse Chemokine Array Kits (R&D Systems, Minneapolis, MN) according to the manufacturer's protocol. For lysates, tumors were frozen in liquid nitrogen and mechanically pulverized. Organ powder was resolved in Bio-Rad Cell Lysis Buffer (Bio-Rad, Hercules, CA) and centrifuged at 13,000×g for 30 minutes. Supernatant was collected and stored at -80°C. Protein levels in organ lysates were quantified by Bradford protein assay (Protein Assay Kit, Bio-Rad, Hercules, CA).

Western Blot

For MITF protein levels, cells were lysed after 48 hours of culture using RIPA-Buffer (50 mM Tris/Cl, 150 mM NaCl, 1 mM EDTA, 1% NP-40, 0.25% Na-DOC, 0.1% Protease Inhibitor, pH 7.4). Protein concentration was quantified by Bradford protein assay (Protein Assay Kit, BioRad, Hercules, CA). The lysates were run on a 10% polyacrylamide gel. MITF was detected using anti-MITF (clone

Table 1. Sequences of all primers for RT-PCR used in this study.

Gene	Sequence	Accession Code	Position
CCL1 murine	L: ccctgaagttatccagtrta R: gcagtttctctacctttgtrca	NM_011329.3	L: 195-217 R: 268-290
CCL2 murine	L: catccacgtgtggctca R: gatcatcttctggrgaatgagt	NM_011333.3	L: 139-156 R: 192-214
CCL3 murine	L: tgcctctctctctctctct R: gtggaatcttccggctgtag	NM_011337.2	L: 119-138 R: 212-231
CCL4 murine	L: gcctctctctctctctct R: ggaggctcagagccatt	NM_013652.2	L: 98-117 R: 154-171
CCL5 murine	L: tgcagaggactctgagacagc R: gagggtgtccgagccata	NM_013653.3	L: 3-23 R: 133-151
CCL6 murine	L: tctttacttctgtgctgtcc R: tggagggttatagcagcat	NM_009139.3	L: 175-195 R: 238-257
CCL7 murine	L: ttctgtgctgctgctcata R: ttgacatagcagcatgtggat	NM_013654.3	L: 92-111 R: 162-182
CCL8 murine	L: ttcttgctgctgctcata R: gcaggtgactggagccttat	NM_021443.3	L: 72-91 R: 129-148
CCL9 murine	L: tgggccagatcacacat R: cccatrgaacattcaatttc	NM_011338.2	L: 230-247 R: 299-321
CCL11 murine	L: agactccacagcgttct R: ggcaggaagttggatgga	NM_011330.3	L: 140-158 R: 214-231
CCL12 murine	L: ccatcagrtctcaggtattgg R: cttccggactggaattctct	NM_011331.2	L: 100-120 R: 175-194
CCL13 murine	L: gcactctctgctctctgg R: atgtaaggcgagaaatgagg	NM_010779.2	L: 61-80 R: 121-140
CCL17 murine	L: tgcctctgggactttctg R: gaatggccctttgaaftaa	NM_011332.3	L: 84-103 R: 157-176
CCL19 murine	L: tgtgctgctctcagattat R: agtcttccgcatcattagcac	NM_011888.2	L: 164-183 R: 265-285
CCL20 murine (var1)	L: aactgggtgaaaaggctgt R: gtccaattccatcccaaaaa	NM_016960.2	L: 299-318 R: 299-318
CCL21a murine	L: tccaagggctcgaagaga R: tgaagtctggtgggatct	NM_011124.4	L: 428-445 R: 501-519
CCL22 murine	L: tcttctgtrggcaattcaga R: gaggtgacggatgtagtcc	NM_009137.2	L: 72-91 R: 144-163
CCL24 murine	L: gcagcatcttcccaagg R: gcagttggggtcagtagaca	NM_019577.4	L: 235-252 R: 291-309
CCL25 murine (var1)	L: gagtgccaccctaggtcatc R: ccagtggtgcttactctga	NM_009138.3	L: 496-515 R: 563-582
CCL26 murine	L: gcaccagtgacgtrtgata R: tgaatctctgaccaccttg	NM_001013412.2	L: 167-186 R: 231-250
CCL27a murine (var1)	L: ggaagcggaggaggat R: cttgtggagacatcggactc	NM_001048179.1	L: 89-106 R: 161-181
CCL28 murine	L: cagagagctgacgggact R: gggctgatgcagatttctta	NM_020279.3	L: 208-226 R: 261-281
CXCL1 murine	L: gactcagccacactccaac R: tgacagcgcagctcattg	NM_008176.3	L: 39-58 R: 150-167
CXCL2 murine	L: aaaatcatcaaaaagataactgaaca R: ctttggttcttccrtgagg	NM_009140.2	L: 308-333 R: 379-398
CXCL3 murine	L: cccaggttcagataatca R: tctgatttagaattgagctctt	NM_203320.2	L: 317-336 R: 404-426
CXCL4 murine	L: tggatccatcttaagcaca R: ccattctcagggtggctat	NM_019932.4	L: 303-322 R: 376-395
CXCL5 murine	L: agagcccaatctccacac R: gagctggagctcattgtg	NM_009141.2	L: 73-92 R: 141-159
CXCL7 murine	L: gccacttcataactccag R: ggtccatgccaatcagatt	NM_023785.2	L: 129-148 R: 204-222
CXCL 9 murine	L: ctttctcttgggcatcat R: gcatcgtgattccttatca	NM_008599.4	L: 72-91 R: 127-146
CXCL10 murine	L: gctgctcattttctgc R: tctcactggcccgtcatc	NM_021274.1	L: 53-70 R: 146-163
CXCL11 murine	L: gctgctgagatgaacaggaa R: ccctgtrttgaacataaggaagc	NM_019494.1	L: 55-74 R: 125-146
CXCL12 murine (var1)	L: ccaactgtgcccttcagat R: attcgggtcaatgcacact	NM_021704.3	L: 278-297 R: 328-347
CXCL13 murine	L: tgggctcagcacagcaa R: atggctccagaataccg	NM_018866.2	L: 34-51 R: 92-110
CXCL14 murine	L: gacagcggcaggagcac R: tttcaagcacgcctctctc	NM_019568.2	L: 209-226 R: 265-283
CXCL15 murine	L: tgcctcaaggctgtrccat R: gacatcgtgcttctgagtrca	NM_011339.2	L: 43-60 R: 106-128
CXCL16 murine	L: tgaactggtgactgctttgagc R: gcaaatgttttgggtgga	NM_023158.6	L: 801-823 R: 858-877
CXCL17 murine	L: tgttgcttccagrtgctc R: ctaggagccaggtttggtc	NM_153576.2	L: 135-154 R: 206-225

TABLE 1 (continued)

Gene	Sequence	Accession Code	Position
XC1L murine	L: agacttctcctcctgactttcct R: gacttcagccccacacctt	NM_008510.1	L: 24-46 R: 79-98
CX3CL1 murine	L: catccgctatcagctaaacca R: cagaagcgtctgrgctgrgt	NM_009142.3	L: 229-249 R: 287-306
HPRT murine	L: cctcctcagaccgcttttt R: aacctggttcatcatcgctaa	NM_013556.2	L: 105-123 R: 175-195
CCL1 human	L: ttgctgctagctgggatgt R: ctggagaagggtacctgcat	NM_002981.2	L: 103-121 R: 148-167
CCL2 human	L: agtctctgccgccctct R: grgactggggcattgattg	NM_002982.3	L: 79-96 R: 153-171
CCL3 human	L: tgcaaccagttctctgcatc R: aatctgccgggaggtgta	NM_002983.2	L: 154-173 R: 211-228
CCL3L1 human	L: tctgcaaccaggctcctct R: tgtcgggagggtgtagctga	NM_021006.5	L: 135-154 R: 192-210
CCL3L3 human	L: tctgcaaccaggctcctct R: tgtcgggagggtgtagctga	NM_001001437.3	L: 125-144 R: 182-200
CCL5 human	L: tgccacatcaaggatattt R: ctttcgggtgacaaagacg	NM_002985.2	L: 200-220 R: 254-272
CCL7 human	L: gaaagcctctcagcacttc R: aatctgtagcagcaggtattgaa	NM_006273.3	L: 78-97 R: 165-188
CCL8 human	L: ccctcagggacttgctcag R: tctccagcctctgtaggga	NM_005623.2	L: 509-527 R: 584-603
CCL13 human	L: acctcaacatgaaagtctctgc R: ggacgtrtgatgcatctgg	NM_005408.2	L: 67-89 R: 148-166
CCL14 human	L: cgtcagcggattatggatta R: eegrttggatcacagcggaaag	NM_032962.4	L: 263-283 R: 341-360
CCL15 human	L: cctctcctgctcatgctt R: cagtggaagctttgacatcatta	NM_032965.5	L: 567-585 R: 638-660
CCL16 human	L: gccctgtctctctctgtct R: gttcaccactcaggaaactttt	NM_004590.3	L: 95-114 R: 151-172
CCL17 human	L: gggagagctgaattcaaaacc R: ggcagcatctctcagttg	NM_002987.2	L: 48-68 R: 136-153
CCL18 human	L: atggccctctgctctgct R: aatctgccaggaggtatagacg	NM_002988.3	L: 114-131 R: 167-188
CCL19 human	L: gcctgctggtttctctggac R: ggtatgggtttctgggtcac	NM_006274.2	L: 161-179 R: 235-253
CCL20 human (var1)	L: atgtgctgtaccaagatttgc R: tcaaagtgtctctgctctc	NM_004591.2	L: 71-92 R: 143-162
CCL21 human	L: tctaccacagacatggctcagt R: agtctgagccccctccat	NM_002989.2	L: 73-94 R: 158-175
CCL22 human	L: cgtgggaaacacttctactgg R: ccttatccctgaaggtagcaa	NM_002990.4	L: 178-199 R: 233-254
CCL23 human (var1)	L: caccagagagatgaaggtct R: catcatgaaactctgctctgcat	NM_145898.3	L: 62-81 R: 148-170
CCL25 human (var1)	L: cctggatgctcgaataagg R: ttggagtttccagaaactcaact	NM_005624.3	L: 378-397 R: 457-479
CCL27 human	L: ctctgagcccagacccta R: gctgagtagcagcaggcagtg	NM_006664.2	L: 105-123 R: 149-168
CCL28 human	L: gagctgatgggatttggac R: cacagattctctgctgctg	NM_148672.2	L: 228-247 R: 271-290
Comp. Factor D human	L: tccaagcctctgtacgac R: gtrggtccctctccgaca	NM_001928.2	L: 296-313 R: 384-401
CXCL1 human	L: tctgcatccccatagtta R: cttcaggaaacagccaactg	NM_001511.2	L: 340-359 R: 425-444
CXCL2 human	L: cccatggttaagaaatcatcg R: cttcaggaaacagccaact	NM_002089.3	L: 431-452 R: 506-525
CXCL3 human	L: gaaatcatcgaaaagatactgaaca R: ggtaagggcagggaccac	NM_002090.2	L: 444-469 R: 537-554
CXCL4 human	L: agcctggagggtgcaagg R: ccattctctcagctggctat	NM_002619.3	L: 340-358 R: 388-407
CXCL5 human	L: ggtcctctgagctcctgt R: acgcagctctctcaacag	NM_002994.4	L: 185-203 R: 273-292
CXCL6 human	L: grccttgggctcctgt R: gtcagcacagcagagacagg	NM_002993.3	L: 233-250 R: 310-329
CXCL7 human	L: ttgctgctgactgctctgg R: gcatacaagtcactgtctgactttcc	NM_002704.3	L: 170-187 R: 237-263
CXCL9 human	L: ccttaacaatttggcccaag R: ttgaaactcattctcagtrtagc	NM_002416.1	L: 183-203 R: 232-255
CXCL10 human	L: gaaaagcagtttagcaaggaaaggt R: gacatatactccatgtagggaaagta	NM_001565.3	L: 363-385 R: 469-494
CXCL11 human	L: agtrtgaaggcatggcta R: tctttgaaactggggagac	NM_005409.4	L: 214-232 R: 272-291
CXCL12 human	L: ccaactgtgcccctcagat R: ctttagcttgggtcaatgc	NM_001178134.1	L: 249-268 R: 304-323

(continued on next page)

TABLE 1 (continued)

Gene	Sequence	Accession Code	Position
CXCL13 human	L: tctctgcttctcatgctgct R: tcaagcttgrtaatagacctcca	NM_006419.2	L: 97-116 R: 149-172
CXCL14 human	L: aagctggaatgaagccaaa R: tgacctcggtacctggacac	NM_004887.4	L: 622-641 R: 688-707
CXCL16 human	L: ttctatgtgctgtgcaagag R: caggtatataatgaaccggcaga	NM_022059.2	L: 1255-1275 R: 1309-1331
CXCL17 human	L: accgaggccaggcttcta R: gggctctcaggaaaccaatct	NM_198477.2	L: 317-334 R: 375-394
gp130 human	L: aggaccaaagatgcctcaac R: gaatgaagatcgggtggatg	NM_002184.3	L: 1097-1116 R: 1146-1165
iL-16 human	L: ggaaggctccctacacg R: caccagctgcaagatttc	NM_004513.5	L: 1865-1882 R: 1960-1978
XCCL1 human	L: cactctctgtcacagctca R: tctgagacttcaactccctacacc	NM_002995.2	L: 132-151 R: 226-248
XCCL2 human	L: actctcctgcacagctcag R: tgagacttcaactccctacacctt	NM_003175.3	L: 1-20 R: 92-114
MITF human (var5)	L: agggagctcacagagctgaa R: tgrtaaatcttctctcgrtcaatc	NM_198158.2	L: 681-702 R: 752-775
GAPDH human (var1)	L: agccacatcgtcagacac R: gcccaatcagccaaatcc	NM_002046.5	L: 169-187 R: 216-234

D5, ThermoFisher Scientific, 1:1000) and secondary mouse monoclonal IgG HRP-conjugated antibody (clone HAF007, R&D Systems, 1:2000). β -Actin mouse monoclonal IgG HRP-conjugated antibody (clone C4, Santa Cruz Biotechnology, Santa Cruz, CA; 1:3000) was used as a loading control. Chemiluminescence was measured using Thermo Scientific Super Signal West Pico PLUS Chemiluminescent Substrate (ThermoFisher Scientific, Waltham, MA) with ChemiDoc Imaging Systems (BioRad). Densitometry was performed with Image Lab Software (BioRad).

Semiquantitative Real-Time PCR

Chemokine mRNA in tumor cell lines and tumor lysates was quantified by real-time PCR. RNA from single cell suspensions or tumor lysates was extracted using Trizol Reagent (Life Technologies, Carlsbad, CA) and quantified with the NanoDrop instrument (ThermoFisher Scientific). Reverse transcription of RNA into cDNA was performed with the RevertAid First Strand cDNA Synthesis Kit (Fermentas, St. Leon-Rot, Germany). Chemokine cDNA copies were quantified by real-time PCR and were normalized to HPRT or GAPDH. Real-time PCR was performed with the LightCycler 480 instrument (Roche) using the LightCycler 480 Probes Master. Primers were designed with the Roche Universal ProbeLibrary Assay Design Center and used with the matching probes from the Universal ProbeLibrary Set (Roche, Basel, Switzerland). The primers used for qRT-PCR are listed in Table 1.

In Vitro Migration Assay

Immune cell migration assays were performed using Corning Transwell Plates (3.0 μ m pore size). Cell-free culture supernatants of human or murine melanoma cells were collected after 48 hours of culture and transferred into the lower chamber. A total of 10^6 freshly isolated human PBMCs or murine splenocytes were resuspended in T cell medium or in RPMI with 0.5% BSA, respectively, and loaded into the upper chamber of the Transwell plates. Migration was allowed for 6 hours at 37°C. After removing the Transwell inserts, cells in the lower chamber were analyzed by flow cytometry. Absolute numbers of migrated cells were calculated by addition of CountBright Absolute Counting Beads (LifeTechnologies).

Transduction of MITF

All constructs were generated by overlap extension PCR and recombinant expression cloning into the retroviral pMP71 vector, as follows: The retroviral vector pMP71 (kindly provided by C. Baum, Hannover) was used for transfection of the ecotropic packaging cell line Plat-E for transduction of murine cell line YUMM1.1 and the packaging cell line Plat-A for the human cell lines. Transduction protocols have been described in detail before [24]. In brief, the packaging cell lines Plat-E or Plat-A were transfected with an MITF-linker-GFP construct, where the linker 2A-sequence was noncleaving through deletion of two amino acids. This allowed to confirm nuclear expression of MITF by confocal microscopy. The produced retrovirus was used to transduce YUMM1.1-, WM8-, and WM35-cells. Transduction efficacy for MITF was controlled by qRT-PCR. The human MITF-M transcript variant 5 (Plasmid #38131, Addgene, Cambridge, MA) was used for transduction of both murine and human cell lines.

Statistics

Statistical analysis was performed with GraphPad Prism Software. Significance was analyzed with unpaired Student's *t* test or, for tumor growth, with two-way ANOVA with Bonferroni correction. Error bars indicate SEM.

Results

MITF Knockdown and Immune Cell Infiltration in Murine B16F10 Melanoma

MITF knockdown has been shown to affect secretion of defined cytokines and chemokines from melanoma cells [12,17]. We performed siRNA-mediated knockdown of MITF on B16F10 melanoma cells (Figure 1A), which highly express MITF at baseline, and analyzed mRNA expression of C-C and C-X-C motif chemokines (Supplementary Figure 1A). MITF knockdown was confirmed with Western blot (Supplementary Figure 1B). Chemokine mRNA levels changed in B16F10 cells upon transfection with siRNA targeting MITF (siMITF) as compared to a siRNA control (siControl). CCL17, CCL25, and CXCL4 were upregulated in MITF knockdown B16F10 cells, whereas CCL5 and CXCL10, highly expressed at

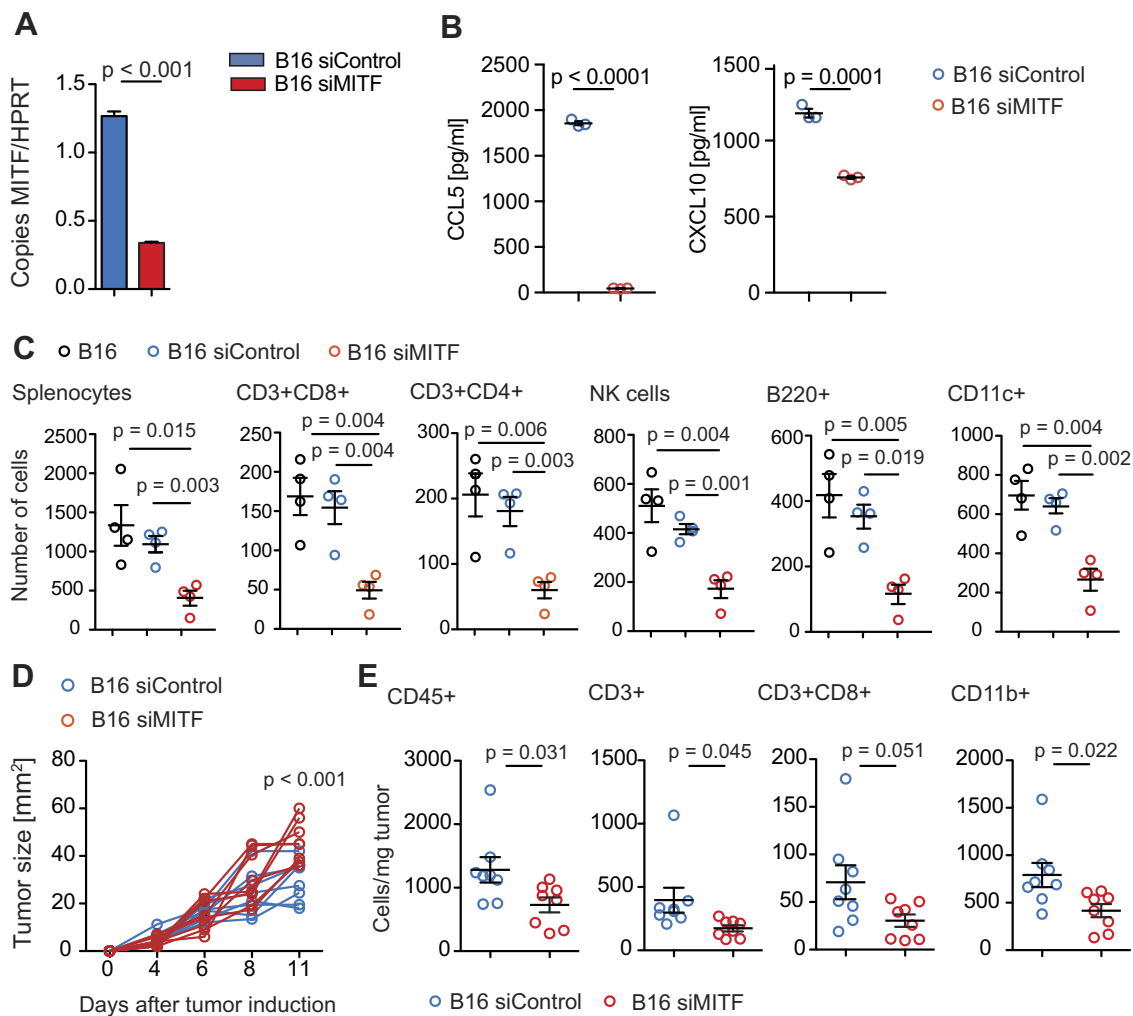


Figure 1. MITF knockdown in B16F10 melanoma results in altered chemokine levels and immune cell attraction. (A) B16F10 cells were transfected with siControl or MITF siRNA. Bars display MITF copies per HPRT as determined by quantitative RT-PCR. (B) Levels of CCL5 and CXCL10 in supernatants of transfected B16F10 cells were analyzed after 48 hours of culture by chemokine ELISA. (C) A total of 10^6 C57BL/6 splenocytes were allowed to migrate for 6 hours towards supernatants or RPMI 0.5% BSA and analyzed by flow cytometry. Dots indicate migrated cells per well. (D, E) C57BL/6 mice were injected with 2.5×10^5 B16F10 cells transfected with siControl ($n = 8$) or MITF siRNA ($n = 8$). (D) Tumor growth over time is displayed. Tumors were harvested on days 11 or 15, and immune cells were analyzed by flow cytometry. (E) Cells per mg tumor are displayed. Panels A to C are representative of three independent experiments. Panels D and E are pooled from two independent experiments.

baseline levels, were significantly downregulated both on mRNA (Supplementary Figure 1A) and on protein level (Figure 1B). We next analyzed the effects of MITF knockdown on immune cell migration towards melanoma cells. *In vitro*, migration of various immune cell subtypes towards supernatants of siMITF-transfected B16F10 cells was reduced as compared to siControl-transfected cells (Figure 1C). In fact, reduction of CD8+ and CD4+ T cells, NK cells, B cells, and CD11c+ dendritic cells (DCs) was most pronounced. *In vivo*, siMITF-transfected B16F10 cells showed an accelerated growth rate as compared to control-transfected B16F10 cells (Figure 1D). Quantification of tumor-infiltrating immune cells recapitulated *in vitro* observations, showing lower recruitment of immune cells to the tumor site; overall numbers of CD45+ cells as well as numbers of CD3+ T cells and CD11b+ myeloid cells in MITF knockdown tumors were reduced (Figure 1E). The number of DC and NK cells remained unchanged (Supplementary Figure 1C). Our *in vitro* results were further confirmed by analyzing protein levels of

intratumoral chemokines; CXCL10 was reduced in siMITF-transfected tumors. In addition, CCL6, CCL8, CCL9/10, CCL12, CCL21, CCL22, CCL27, CCL28, CXCL1, CXCL9, CXCL11, and CX3CL1 were strongly reduced in siMITF-transfected tumors as compared to controls (Supplementary Figure 1D).

MITF Overexpression in YUMM1.1 Melanoma Cells and In Vitro Immune Cell Migration

We next examined YUMM1.1 melanoma cells, a cell line derived from a genetically engineered mouse model characterized by BRAF activation as well as PTEN and Cdkn2a inactivation, which is considered to mimic characteristics of human melanoma [21]. YUMM1.1 cells express very low levels of MITF at baseline, which make them a suitable tool for MITF overexpression studies. We transduced YUMM1.1 cells with MITF (or GFP as a control) and confirmed overexpression of MITF by qRT-PCR (Figure 2A) and

Western Blot (Supplementary Figure 2B). When analyzing chemokine expression in YUMM1.1 cells, we found that MITF overexpression had no significant influence on CCL2 expression (Supplementary Figure 2C) but particularly led to upregulated CCL5 and CXCL10 expression on mRNA (Supplementary Figure 2A) and protein levels (Figure 2B) as compared to control cells. This was paralleled by increased immune cell migration, specifically, of the lymphocyte populations such as CD8+ and CD4+ T cells, B cells, and NK cells, which was induced by supernatants of MITF-

overexpressing YUMM1.1 cells (Figure 2C). No difference in migration was seen for DC and other CD11b+ myeloid cells (Supplementary Figure 2D).

MITF Overexpression and Tumor Growth in YUMM1.1 Melanomas

Next, we injected MITF-transduced YUMM1.1 cells subcutaneously into mice. Surprisingly, MITF-transduced YUMM1.1 tumors showed accelerated growth as compared to control-transduced cells

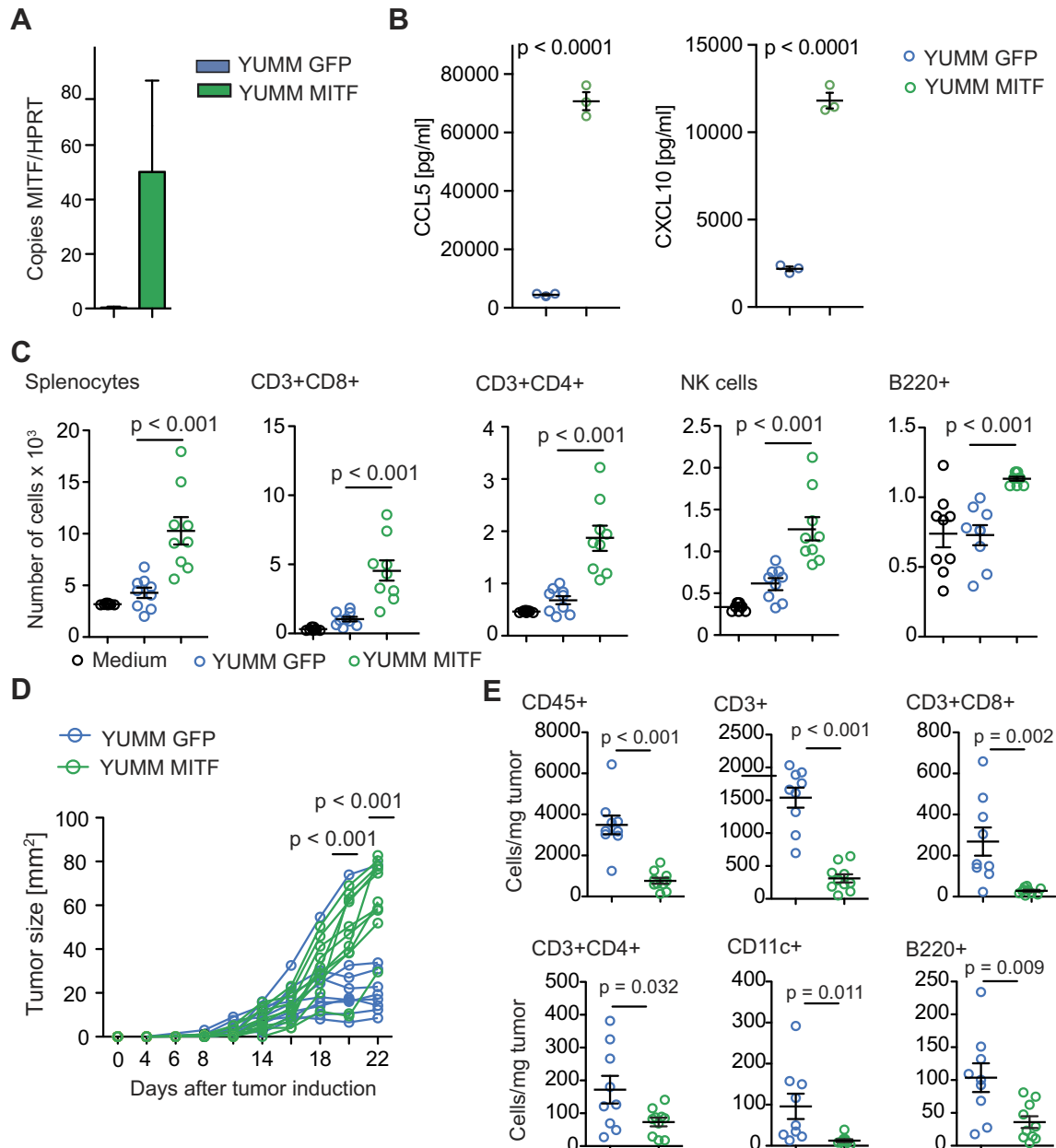


Figure 2. MITF overexpression in YUMM1.1 cells changes chemokine expression and immune cell attraction. (A) Relative MITF mRNA expression of MITF-transduced YUMM1.1 cells. (B) ELISA assay for chemokine detection in supernatants of transduced YUMM1.1 cells was analyzed after 48 hours of culture. (C) A total of 10^6 C57BL/6 splenocytes were allowed to migrate for 6 hours towards YUMM1.1 supernatants or migration medium and analyzed by flow cytometry. Dots indicate migrated cells per well. Three independently collected supernatants were used. (D, E) C57BL/6 mice were injected with 2×10^6 YUMM melanoma cells transduced with MITF ($n = 10$) or with GFP ($n = 9$). (D) Tumor growth over time. Tumors were harvested on days 22 or 27 and analyzed by flow cytometry. (E) Cells per mg tumor. Data are pooled from two independent experiments. Panel B is representative of three independent experiments.

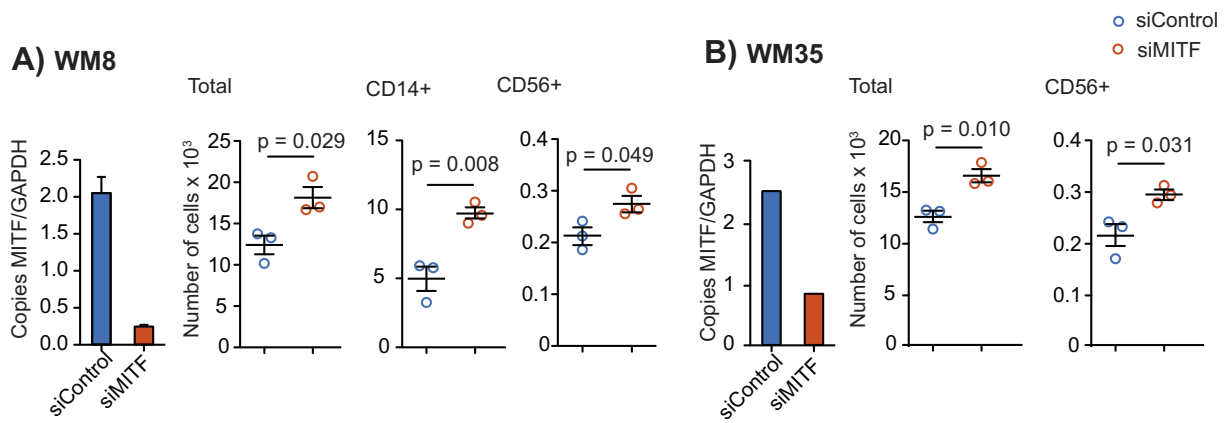


Figure 3. MITF knockdown in human melanoma cell lines WM8 and WM35. (A, B) Human WM8 (A) or WM35 (B) melanoma cells were transfected with control or with MITF siRNA. Knockdown efficiency was confirmed by q-RT-PCR. Copies of MITF per GAPDH are displayed. A total of 10⁶ human PBMCs were transferred into the upper well of a Transwell migration system; lower wells were loaded with WM8 or WM35 supernatants or migration medium. Cells were left to migrate for 6 hours, and migrated cells were analyzed by flow cytometry. Dots indicate migrated cells per well. Data are representative of at least three independent experiments.

(Figure 2D). When analyzing tumor infiltrating immune cells, we observed that the *in vivo* phenotype closely resembled the phenotype we had observed in MITF knockdown B16F10 tumors. The number of total CD45+ cells as well as of CD8+ T cells and CD4+ T helper

cells was decreased, while the numbers of CD11b+ myeloid cells and NK cells remained unchanged (Figure 2E and Supplementary Figure 2E). In contrast to the B16 model, numbers of B220+ B cells and CD11c+ DC were also decreased in MITF-transduced YUMM1.1

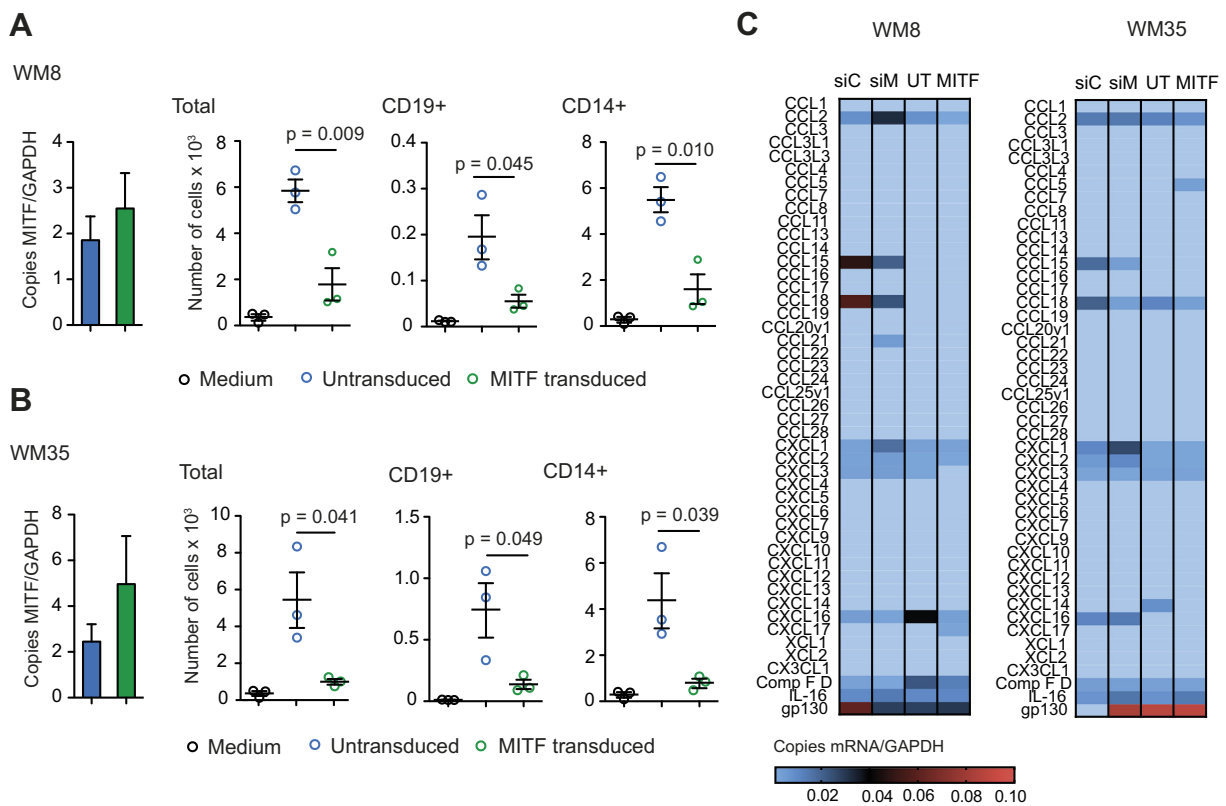


Figure 4. MITF overexpression in human melanoma cell lines WM8 and WM35. (A, B) Relative MITF mRNA expression of MITF-transduced WM8 (A) or WM35 (B) melanoma cells. MITF expression was confirmed by qRT-PCR. A total of 10⁶ human PBMCs were transferred into the upper well of a Transwell migration system; lower wells were loaded with WM8 or WM35 supernatants or migration medium. Cells were left to migrate for 6 hours, and migrated cells were analyzed by flow cytometry. Dots indicate migrated cells per well. Data are representative of three independent experiments. (C) Chemokine mRNA per GAPDH in MITF-transduced (MITF) and MITF knockdown (siMITF) WM8 and WM35 cells relative to control condition (siC, siControl; UT, untransduced). Data are pooled from three independent experiments.

tumors (Figure 2E). When analyzing intratumoral chemokine levels, we found that mRNA expression of most chemokines in MITF-transduced tumors remained unchanged or was reduced when compared to control tumors (Supplementary Figure 2F). This included CCL5 and CXCL10, which we had found upregulated in MITF-transduced YUMM1.1 cells *in vitro* (Supplementary Figure 2F).

MITF in Human Melanoma Cells and Immune Cell Migration

We next sought to determine the role of MITF expression levels in human melanoma cells. We investigated WM8 and WM35 melanoma cell lines, both known to express intermediate baseline levels of MITF. This allows performing knockdown and overexpression studies within the same cell line. MITF knockdown was performed with siRNA and was confirmed by qPCR (Figure 3, A and B) and Western Blot (Supplementary Figure 3, A and B). MITF knockdown resulted in an increased migration of peripheral blood mononuclear cells (PBMC), more specifically of CD56+ NK cells, towards tumor cell supernatants of both WM8 and WM35 cells (Figure 3, A and B). For WM8 cells, an increased migration of CD14+ monocytes towards tumor cell supernatant was observed (Figure 3A). There were no consistent changes in the migration of T or B cells towards MITF-silenced supernatants of WM8 or WM35 cells, with increased migration of CD4+ T cells in only 1 out of 3 experiments (Supplementary Figure 3, C and D). MITF overexpression in WM8 and WM35 cells was confirmed by qPCR (Figure 4, A and B) and Western Blot (Supplementary Figure 4, A and B). MITF overexpression resulted in reduced migration of CD14+ myeloid cells and CD19+ cells towards tumor supernatants (Figure 4, A and B). When analyzing chemokine expression levels in WM8 and WM35 cells upon MITF siRNA knockdown or MITF overexpression, we found a comparable expression pattern in both tumor cell lines; MITF knockdown resulted in increased expression of CCL2; CXCL1; and, in WM8 cells only, of CXCL2, whereas levels of CCL15 and CCL19 were reduced in both cell lines. *Vice versa*, MITF overexpression mostly decreased expression of chemokines, *e.g.*, CCL18, CXCL14, and CXCL16 (Figure 4C).

Discussion

We have analyzed the influence of MITF on melanoma cell chemokine expression and immune cell attraction. Unexpectedly, MITF was found to have opposing effects on chemokine expression in murine and human melanoma cells: In the murine cell lines, MITF knockdown resulted in reduced immune cell attraction, while MITF overexpression consistently resulted in increased immune cell migration. The exact opposite was observed in the human melanoma cell lines analyzed. We assume that this may be due to differences in genetic backgrounds, driver mutations of the melanoma cell lines, and diverging underlying mutations rather than to species-specific differences. Gene expression differences between murine and human melanoma cell lines have been described before [25]. For example, it is known that loss of PTEN, as for the YUMM1.1 cell line, mediates an immunosuppressive phenotype associated with decreased T cell infiltration [26]. Moreover, BRAF mutations have previously been reported to influence MITF transcription [27]. A more extensive analysis of different human and murine melanoma cell lines combined with an in-depth study of genomic mutations and

their interactions with MITF will be necessary to answer the observed differences of human and murine melanoma cell lines.

Chemokine expression patterns and immune cell subtypes attracted to the tumor cells also differed between the murine and human melanoma models: murine cell lines mostly attracted lymphoid cell types, whereas human cell lines preferentially attracted CD14+ monocytic cells. This is in line with previous reports, according to which B16F10 tumors are marked by a dominantly lymphoid cell infiltration, whereas human melanomas induce migration of myeloid cells [17,28]. Also in pancreatic cancer, different immune cell infiltrates in mice and humans have been reported: murine models are dominated by inhibitory myeloid cell infiltrates, while in humans, pancreatic adenocarcinomas T cells are highly prevalent [29]. Despite many conserved mechanisms and pathways, differences exist between the human and the murine immune system, including surface receptor expression, chemokine expression, and functional aspects of immune cell populations [30].

Interestingly, only few chemokines were expressed on mRNA level in the two murine cell lines studied. Of those, only CXCL10 was considerably reduced in MITF-deficient B16F10 cells. Strikingly, CXCL10 and CCL5 were upregulated in MITF-transduced YUMM1.1 melanoma cells. These chemokines are known to recruit T and NK cells to tumors *via* CCR5 and CXCR3. In CXCR3-KO mice, B16F10 tumors have decreased infiltration with CD8+ T cells and reduced survival of mice [31–33]. Intratumoral CCL5 has also been reported to play a role in melanoma progression, with melanoma cell-intrinsic CCR5 expression [34,35]. It would be interesting to further dissect the role of MITF-regulated expression of these chemokines in melanoma.

In the human melanoma cell lines investigated in this study, MITF siRNA knockdown led to an increased migration of CD14+ monocytic cells, whereas overexpression of MITF showed opposing effects. These findings are in line with a recent study reporting the recruitment of CD14+ cells into MITF^{low} human melanomas [17]. In this study, murine MITF^{low} cell lines showed a high infiltration with CD14+ myeloid cells linked to a high expression of CCL2, CCL5, and CXCL10. In contrast to our study however, MITF^{low} cell lines were directly compared to MITF^{high} cell lines, which did not allow for assessing acute changes of MITF levels within the same cell line. In our human melanoma cells, chemokine arrays showed an induction of CCL2 upon MITF knockdown, which is in line with current studies describing the CCL2-MITF axis as a component of the senescence-related secretome [12,17]. We also observed increased levels of CXCL1 in MITF-knockdown human melanoma cells. CXCL1 is known to be critically involved in melanoma development, angiogenesis, and growth [36,37]. MITF has been demonstrated to bind the CXCL1 promoter region in chromatin immunoprecipitation assays [38].

In our *in vivo* models, we observed reduced numbers of T cells and myeloid cells in MITF-knockdown B16F10 tumors concurrent with higher tumor growth. Surprisingly, MITF-transduced YUMM1.1 cells also showed accelerated tumor growth, and we found decreased intratumoral immune cell numbers. This is in contrast to the observed increase in immune cell attraction to MITF-transduced YUMM1.1 cells *in vitro*. When analyzing intratumoral chemokine levels, we found these diverging from *in vitro* tumor cell chemokine expression: overall chemokine levels were lower in both MITF-knockdown and MITF-transduced tumors. The opposing findings *in vitro* and *in vivo* for the YUMM1.1 cell line may be attributed to the

tumor environment where, in contrast to cell culture, stromal and immune cells contribute to chemokine production. While we can clearly demonstrate *in vitro* how changes in MITF levels affect chemokine levels in and immune cell attraction to melanoma cells, the complexity of the tumor microenvironment *in vivo* seems to overcome the *in vitro* effects, at least in the YUMM1.1 model. Several explanations are possible for the discrepancy of our *in vitro* and *in vivo* observations: tumor-associated immune cells might contribute to a high extent to intratumoral chemokine levels and thereby influence the tumor microenvironment; interactions with the tumor microenvironment as well as the high growth rate might affect the biology of YUMM1.1 tumor cells *in vivo*, modifying chemokine secretion; or immune cell-mediated selective pressure might lead to the domination of MITF low tumor cells *in vivo*. These results shed further light on the discrepancies in the consequences of different MITF levels for patient's prognosis. While higher or lower levels of MITF might have opposing consequences on the melanoma cells themselves, the impact on the environment will differ as well, thus potentially compensating or reverting function of MITF levels on disease outcome. Our data clearly show that changes in MITF levels influence the tumor microenvironment by suppressing immune cell migration to or accumulation at the tumor site and, thus, leading to an increased tumor growth. This is of importance since BRAF inhibitors, which are currently used for melanoma treatment, influence intratumoral MITF levels [39].

It is hard to define the exact role for MITF in shaping the immunological tumor microenvironment because of differing interactions with melanoma driver mutations in different melanoma cell lines (such as BRAF mutations, which are highly prevalent in human melanomas but only present in the YUMM1.1 cell line). Moreover, the kinetics of dynamic effects, as compared to stably decreased levels of MITF, may play a role in our knockdown and overexpression experiments. In our studies, we have both observed divergencies between *in vitro* and *in vivo* findings as well as divergencies between human and murine melanoma cell lines. We believe that melanomas of different origin, endowed with diverging underlying mutations and variable MITF expression at steady state, will react differently to transient changes in MITF levels. A detailed study of a higher number of different melanomas and their interactions with the immune system will be necessary to depict effects of MITF levels in different contexts. Nevertheless, our results show that MITF clearly influences chemokine expression and immune cell attraction in different murine and human melanomas.

Since the emergence of checkpoint blockade has revolutionized melanoma therapy in the past years [14,40] it has become more and more important to understanding the factors which regulate melanoma immunogenicity and immune cell infiltration. Our study provides a first step to understanding how MITF might influence the interaction of melanoma cells with immune cells and might provide a basis for further therapeutic interventions in combination with targeted immunotherapies.

Supplementary data to this article can be found online at <https://doi.org/10.1016/j.tranon.2018.10.014>.

Acknowledgements

We thank Dr. Bosenberg (Yale University, USA) for providing the YUMM1.1 cell line.

This study was supported by grants from the international doctoral program "i-Target: Immunotargeting of cancer" funded by the Elite

Network of Bavaria (to S.K. and S.E.), the Melanoma Research Alliance (grant number 409510 to S.K.), the Marie-Sklodowska-Curie "Training Network for the Immunotherapy of Cancer (IMMUTRAIN)" funded by the H2020 program of the European Union (to S.E. and S.K.), the Else Kröner-Fresenius-Stiftung (to S.K.), the German Cancer Aid (to S.K.), the Ernst-Jung-Stiftung (to S.K.), the LMU Munich's Institutional Strategy LMU excellent within the framework of the German Excellence Initiative (to S.E. and S.K.), the Bundesministerium für Bildung und Forschung VIP+ grant ONKAT-TRACT (to S.E. and S.K.), the European Research Council Starting Grant (grant number 756017 to S.K.), the German Research Foundation (DFG) (to P.D.), and the CIPS-M women grant (to G.M.W.).

Conflict of Interest Statement

The authors declare that no potential conflicts of interest exist. Parts of this work have been performed as parts of the doctoral theses of C. A., A. K., and B. C. at the Ludwig-Maximilians-Universität München, Germany.

References

- [1] Garraway LA, Widlund HR, Rubin MA, Getz G, Berger AJ, Ramaswamy S, Beroukhi R, Milner DA, Granter SR, and Du J, et al (2005). Integrative genomic analyses identify MITF as a lineage survival oncogene amplified in malignant melanoma. *Nature* **436**(7047), 117–122.
- [2] King R, Googe PB, Weilbaeher KN, Mihm Jr MC, and Fisher DE (2001). Microphthalmia transcription factor expression in cutaneous benign, malignant melanocytic, and nonmelanocytic tumors. *Am J Surg Pathol* **25**(1), 51–57.
- [3] Cheli Y, Ohanna M, Ballotti R, and Bertolotto C (2010). Fifteen-year quest for microphthalmia-associated transcription factor target genes. *Pigment Cell Melanoma Res* **23**(1), 27–40.
- [4] Ugurel S, Houben R, Schrama D, Voigt H, Zapotka M, Schadendorf D, Bröcker EB, and Becker JC (2007). Microphthalmia-associated transcription factor gene amplification in metastatic melanoma is a prognostic marker for patient survival, but not a predictive marker for chemosensitivity and chemotherapy response. *Clin Cancer Res* **13**(21), 6344–6350.
- [5] Van Allen EM, Wagle N, Sucker A, Treacy DJ, Johannessn CM, Goetz EM, Place CS, Taylor-Weiner A, Whittaker S, and Kravkov GV, et al (2014). The genetic landscape of clinical resistance to RAF inhibition in metastatic melanoma. *Cancer Discov* **4**(1), 94–109.
- [6] Muller J, Krijgsman O, Tsoi J, Robert L, Hugo W, Song C, Kong X, Possik PA, Cornelissen-Steijger PD, and Geukes Foppen MH, et al (2014). Low MITF/AXL ratio predicts early resistance to multiple targeted drugs in melanoma. *Nat Commun* **5**, 5712.
- [7] Beuret L, Flori E, Denoyelle C, Bille K, Busca R, Picardo M, Bertolotto C, and Ballotti R (2007). Up-regulation of MET expression by alpha-melanocyte-stimulating hormone and MITF allows hepatocyte growth factor to protect melanocytes and melanoma cells from apoptosis. *J Biol Chem* **282**(19), 14140–14147.
- [8] Hoek KS, Schlegel NC, Brafford P, Sucker A, Ugurel S, Kumar R, Weber BL, Nathanson KL, Phillips DJ, and Herlyn M, et al (2006). Metastatic potential of melanomas defined by specific gene expression profiles with no BRAF signature. *Pigment Cell Res* **19**(4), 290–302.
- [9] Javelaud D, Alexaki VI, Pierrat MJ, Hoek KS, Dennler S, Van Kempen L, Bertolotto C, Ballotti R, Saule S, and Delmas V, et al (2011). GLI2 and M-MITF transcription factors control exclusive gene expression programs and inversely regulate invasion in human melanoma cells. *Pigment Cell Melanoma Res* **24**(5), 932–943.
- [10] Carreira S, Goodall J, Denat L, Rodriguez M, Nuciforo P, Hoek KS, Testori A, Larue L, and Goding CR (2006). Mitf regulation of *Dial1* controls melanoma proliferation and invasiveness. *Genes Dev* **20**(24), 3426–3439.
- [11] Eccles MR, He S, Ahn A, Slobbe LJ, Jeffs AR, Yoon HS, and Baguley BC (2013). MITF and PAX3 play distinct roles in melanoma cell migration; outline of a "genetic switch" theory involving MITF and PAX3 in proliferative and invasive phenotypes of melanoma. *Front Oncol* **3**, 229.

- [12] Ohanna M, Giuliano S, Bonet C, Imbert V, Hofman V, Zangari J, Bille K, Robert C, Bressac-de Paillerets B, and Hofman P, et al (2011). Senescent cells develop a PARP-1 and nuclear factor- κ B-associated secretome (PNAS). *Genes Dev* **25**(12), 1245–1261.
- [13] Strub T, Giuliano S, Ye T, Bonet C, Keime C, Kobi D, Le Gras S, Cormont M, Ballotti R, and Bertolotto C, et al (2011). Essential role of microphthalmia transcription factor for DNA replication, mitosis and genomic stability in melanoma. *Oncogene* **30**(20), 2319–2332.
- [14] Hodi FS, O'Day SJ, McDermott DF, Weber RW, Sosman JA, Haanen JB, Gonzalez R, Robert C, Schadendorf D, and Hassel JC, et al (2010). Improved survival with ipilimumab in patients with metastatic melanoma. *N Engl J Med* **363**(8), 711–723.
- [15] Herbst RS, Soria JC, Kowanzet M, Fine GD, Hamid O, Gordon MS, Sosman JA, McDermott DF, Powderly JD, and Gettinger SN, et al (2014). Predictive correlates of response to the anti-PD-L1 antibody MPDL3280A in cancer patients. *Nature* **515**(7528), 563–567.
- [16] van der Woude LL, Gorris MAJ, Halilovic A, Figdor CG, and de Vries IJM (2017). Migrating into the tumor: a roadmap for T cells. *Trends Cancer* **3**(11), 797–808.
- [17] Riesenber S, Groetchen A, Siddaway R, Bald T, Reinhardt J, Smorra D, Kohlmeyer J, Renn M, Phung B, and Aymans P, et al (2015). MITF and c-Jun antagonism interconnects melanoma dedifferentiation with pro-inflammatory cytokine responsiveness and myeloid cell recruitment. *Nat Commun* **6**, 8755.
- [18] Kamaraju AK, Bertolotto C, Chebath J, and Revel M (2002). Pax3 down-regulation and shut-off of melanogenesis in melanoma B16/F10.9 by interleukin-6 receptor signaling. *J Biol Chem* **277**(17), 15132–15141.
- [19] Smalley KS, Contractor R, Nguyen TK, Xiao M, Edwards R, Muthusamy V, King AJ, Flaherty KT, Bosenberg M, and Herlyn M, et al (2008). Identification of a novel subgroup of melanomas with KIT/cyclin-dependent kinase-4 overexpression. *Cancer Res* **68**(14), 5743–5752.
- [20] Kobold S, Merk M, Hofer L, Peters P, Bucala R, and Endres S (2014). The macrophage migration inhibitory factor (MIF)-homologue D-dopachrome tautomerase is a therapeutic target in a murine melanoma model. *Oncotarget* **5**(1), 103–107.
- [21] Meeth K, Wang JX, Micevic G, Damsky W, and Bosenberg MW (2016). The YUMM lines: a series of congenic mouse melanoma cell lines with defined genetic alterations. *Pigment Cell Melanoma Res* **29**(5), 590–597.
- [22] Larribere L, Hilmi C, Khaled M, Gaggioli C, Bille K, Auburger P, Ortonne JP, Ballotti R, and Bertolotto C (2005). The cleavage of microphthalmia-associated transcription factor, MITF, by caspases plays an essential role in melanocyte and melanoma cell apoptosis. *Genes Dev* **19**(17), 1980–1985.
- [23] Bourseguin J, Bonet C, Renaud E, Pandiani C, Boncompagni M, Giuliano S, Pawlikowska P, Karmous-Benailly H, Ballotti R, and Rosselli F, et al (2016). FANCD2 functions as a critical factor downstream of Mitf to maintain the proliferation and survival of melanoma cells. *Sci Rep* **6**36539.
- [24] Kobold S, Steffen J, Chaloupka M, Grassmann S, Henkel J, Castoldi R, Zeng Y, Chmielewski M, and Schmollinger JC, et al (2015). Selective bispecific T cell recruiting antibody and antitumor activity of adoptive T cell transfer. *J Natl Cancer Inst* **107**(1), 364.
- [25] Nakayama J, Guan XC, Nakashima M, Mashino T, and Hori Y (1997). In vitro comparison between mouse B16 and human melanoma cell lines of the expression of ICAM-1 induced by cytokines and/or hyperthermia. *J Dermatol* **24**(6), 351–360.
- [26] Peng W, Chen JQ, Liu C, Malu S, Creasy C, Tetzlaff MT, Xu C, McKenzie JA, and Zhang C, et al (2016). Loss of PTEN promotes resistance to T cell-mediated immunotherapy. *Cancer Discov* **6**(2), 202–216.
- [27] Wellbrock C, Rana S, Paterson H, Pickersgill H, Brummelkamp T, and Marais R (2008). Oncogenic BRAF regulates melanoma proliferation through the lineage specific factor MITF. *PLoS One* **3**(7)e2734.
- [28] Pachynski RK, Scholz A, Monnier J, Butcher EC, and Zabel BA (2015). Evaluation of tumor-infiltrating leukocyte subsets in a subcutaneous tumor model. *J Vis Exp* **98**.
- [29] Pillarisetty VG (2014). The pancreatic cancer microenvironment: an immunologic battleground. *Oncoimmunology* **3**(8)e950171.
- [30] Mestas J and Hughes CC (2004). Of mice and not men: differences between mouse and human immunology. *J Immunol* **172**(5), 2731–2738.
- [31] Campanella GS, Medoff BD, Manice LA, Colvin RA, and Luster AD (2008). Development of a novel chemokine-mediated in vivo T cell recruitment assay. *J Immunol Methods* **331**(1–2), 127–139.
- [32] Chheda ZS, Sharma RK, and Jala VR (2016). Chemoattractant receptors BLT1 and CXCR3 regulate antitumor immunity by facilitating CD8+ T cell migration into tumors. **197**(5), 2016–2026.
- [33] Martin-Fontecha A, Thomsen LL, Brett S, Gerard C, Lipp M, Lanzavecchia A, and Sallusto F (2004). Induced recruitment of NK cells to lymph nodes provides IFN-gamma for T(H)1 priming. *Nat Immunol* **5**(12), 1260–1265.
- [34] Mrowietz U, Schwenk U, Maune S, Bartels J, Küpper M, Fichtner I, Schröder JM, and Schadendorf D (1999). The chemokine RANTES is secreted by human melanoma cells and is associated with enhanced tumour formation in nude mice. *Br J Cancer* **79**(7–8), 1025–1031.
- [35] Payne AS and Cornelius LA (2002). The role of chemokines in melanoma tumor growth and metastasis. *J Invest Dermatol* **118**(6), 915–922.
- [36] Dhawan P and Richmond A (2002). Role of CXCL1 in tumorigenesis of melanoma. *J Leukoc Biol* **72**(1), 9–18.
- [37] Luan J, Shattuck-Brandt R, Haghnegahdar H, Owen JD, Strieter R, Burdick M, Nirodi C, Beauchamp D, and Johnson KN, et al (1997). Mechanism and biological significance of constitutive expression of MGSA/GRO chemokines in malignant melanoma tumor progression. *J Leukoc Biol* **62**(5), 588–597.
- [38] Botton T, Puissant A, Cheli Y, Tomic T, Giuliano S, Fajas L, Deckert M, Ortonne JP, and Bertolotto C, et al (2011). Ciglitazone negatively regulates CXCL1 signaling through MITF to suppress melanoma growth. *Cell Death Differ* **18**(1), 109–121.
- [39] Aida S, Sonobe Y, Tanimura H, Oikawa N, Yuhki M, Sakamoto H, and Mizuno T (2017). MITF suppression improves the sensitivity of melanoma cells to a BRAF inhibitor. *Cancer Lett* **409**, 116–124.
- [40] Pawelec G (2018). Immune correlates of clinical outcome in melanoma. *Immunology* **153**(4), 415–422.